Collective diffusion in colloidal crystals

Paul A. Rundquist, R. Kesavamoorthy,[a] S. Jagannathan, and Sanford A. Asher[b]
Department of Chemistry, University of Pittsburgh, Pittsburgh, Pennsylvania 15260

(Received 20 June 1991; accepted 23 August 1991)

Electrostatically stabilized colloidal crystals prepared from aqueous suspensions of dyed polystyrene spheres compress locally when illuminated by intense laser light of wavelengths absorbed by the dye. The compression, which derives from the temperature dependence of the interparticle repulsive interaction, results in a concentration gradient where particles diffuse into the illuminated regions. The concentration gradient relaxes when the pump light is removed. We experimentally constrain particle diffusion to one dimension by creating a spatially periodic intensity grating which results in a periodic concentration profile. We measure the relaxation time constant of this concentration grating by monitoring the time-dependent transmitted intensity of a low intensity probe beam when the diffraction conditions are almost satisfied for the probe wavelength. The collective diffusion coefficient is found from the relaxation time constant.

INTRODUCTION

Suspensions of monodisperse polymer spheres are used frequently as model systems to study phases and phase transitions since colloid ordering occurs at macroscopic length scales.[1-6] Aqueous suspensions of charged polystyrene spheres can mimic the gas, liquid, glass, and crystalline phases on a length scale of nanometers to microns.[1,5,7-10] These phases form spontaneously and the stable phase depends on such parameters as the sphere size and surface charge, the particle concentration, the solvent dielectric constant, and the solution ionic strength.[1,7,8,11] The charges on the surface of the spheres derive from the dissociation of strong acid groups which are incorporated during the synthesis. The diffuse counterion cloud extends from the surface into solution and does not completely screen the surface charge. As a result, a net repulsive interaction exists between spheres at particle separation distances of several sphere diameters (hundreds of nanometers). The formation of a regular crystal structure minimizes these repulsive interactions; the lattice parameter is completely determined by the sphere number density. Colloidal crystals diffract light efficiently and have been prepared to diffract near UV, visible, and near IR radiation. The diffraction phenomenology has been examined experimentally and theoretically.[12-15] Highly efficient colloidal crystal optical filters which reject narrow bandwidths of light have been developed and are available commercially.[16-18]

Probing the structure and dynamics of colloidal systems, including colloidal crystals, by laser light scattering is now routine.[11,19] The colloid collective (mutual) and self (tracer)-diffusion is sensitive to interparticle and particle–solvent interactions and can be altered easily by changing the suspension composition or temperature. Collective diffusion describes how a concentration fluctuation relaxes and, hence, is a measure of bulk particle motion over large distances compared to the interparticle separation.[11] Consequently, the collective diffusion coefficient is related to the bulk modulus. Self-diffusion, on the other hand, refers to single-particle motion and is determined by interparticle interactions.[11] In the dilute limit, both the collective and the self-diffusion coefficients approach the free-particle diffusion coefficient. At higher concentrations, such as those particle concentrations necessary for forming a crystalline phase, collective and self-diffusion are distinctly different processes.[11,20-23] Therefore, in order to fully characterize concentrated suspensions, both the collective and self-diffusion coefficients are required.

Quasielastic light scattering is often the technique of choice for monitoring collective and self-diffusion at low-particle concentrations. At higher-particle number densities, however, multiple scattering complicates the analysis. Techniques such as forced Rayleigh scattering have been developed to measure the self-diffusion coefficient.[21,24,25] However, while techniques have been developed to create macroscopic particle concentration gradients, these methods have not been used to measure the collective diffusion coefficient. Radiation pressure, for instance, has been used to induce a particle concentration grating in disordered colloidal suspensions which results in local ordering.[26] In addition, concentration gradients have been induced by application of electric[27-29] and gravitational[30-32] fields, and by centrifugation[33] and shearing.[34-37]

In this report, we present a novel technique to determine the collective diffusion coefficient in colloidal crystals. We create a particle concentration grating and we measure the relaxation time constant. In previous work, we used diffraction techniques to demonstrate that local heating, which derives from the absorption of light by dyes contained within the spheres, results in a compression of the crystal within the heated region.[38,39] We showed that these temperature-induced changes in the crystal lattice parameter derive from the temperature dependence of the electrostatic interparticle repulsive interaction. In this study, the experimental conditions are modified such that the temperature-induced bulk particle motion is constrained to one dimension. We use the photothermal compression phenomenon to create a spatially

[a] Materials Science Division, Indira Gandhi Centre for Atomic Research, Kalpakkam 603102, India.
[b] Author to whom correspondence should be addressed.

 0021-9606/91/238546-06$03.00

periodic particle concentration profile. Close to the diffraction condition, changes in the lattice parameter result in changes in the transmitted intensity. The time-dependent relaxation of the particle concentration grating is determined from transmitted intensity changes. We determine the collective diffusion coefficient from the relaxation time constant.

EXPERIMENTAL

The low incident intensity diffraction properties of the dyed and undyed colloidal crystals used in this study have been reported previously.[12] The crystals were prepared from aqueous suspensions of 83 nm diameter polystyrene spheres (2370 ± 80 charge groups per sphere as determined by suspension conductance as a function of particle concentration[40]) with and without strongly absorbing, nonfluorescing dye (Oil Red O, Aldrich) molecules incorporated in the particles. The procedures used to dye the spheres and construct the crystals have been reported previously.[12,13,16–18,38,39] The structures of the crystals were determined to be body centered cubic (bcc) from their Kossel ring patterns, where the (110) planes are parallel to the quartz plates of the cell.[13,31]

A Perkin–Elmer Lambda 9 UV–visible–near IR spectrophotometer was used to determine the lattice spacing. The wavelength of minimum transmission λ_0 is related to the interplaner spacing by Bragg's law

$$m\lambda_0 = 2n_s d_{hkl} \sin \theta_B^{xtl}, \tag{1}$$

where m is the diffraction order, n_s is the suspension refractive index, d_{hkl} is the interplaner spacing of the bcc (110) planes, and θ_B^{xtl} is the Bragg angle in the crystal. The suspension refractive index n_s was measured at 589.3 nm using a temperature controlled Abbe refractometer and was related to the refractive indices of pure water n_w and polystyrene n_{ps} by

$$n_s = n_w(1-\phi) + n_{ps}\phi, \tag{2}$$

where ϕ is the volume fraction of polystyrene in the suspension. The volume fraction for this crystal is $\phi = 0.0205$. The Cauchy relations[41,42] from which the suspension refractive index at the wavelength of incidence are given by

$$n_w = 1.324 + 3046/\lambda_0^2 \tag{3}$$

and

$$n_{ps} = 1.5683 + 10\,087/\lambda_0^2. \tag{4}$$

A schematic of the experimental apparatus is illustrated in Fig. 1. A Spectra Physics model 164 argon ion laser with a broadband rear reflector was used as the source. The laser output was expanded using two short focal length lenses and dispersed with a diffraction grating. The vertically polarized 514.5 nm pump beam was reflected by a mirror and focused partially with a spherical lens through a Ronchi ruling (100 lines/in. Edmund Scientific). The resultant one-dimensional spatially periodic array of bright spots was imaged with a 44 mm cylindrical lens to create a one-dimensional periodic array of bright fringes. A Newport Model 846HP electronic shutter, controlled by a Newport Model 845 digital shutter controller, was placed before the sample to turn the pump beam on and off and to trigger detection. An aperture after the shutter limited the number of fringes on the sample to ~ 20.

The bright fringe periodicity ($470\ \mu m \pm 4\%$) was determined by translating a razor blade, mounted at the sample position, through the intensity grating. The height of the bright fringes at the sample was determined to be 2 mm. The incident power density per fringe was determined using a Scientech model 361 laser power meter.

Neutral density filters were used to decrease the intensity of the 488 nm probe beam. A 300 mm focal length lens focused the probe beam on the sample. The spot size at the sample was determined to be less than $50\ \mu m$ in diameter by translating a razor blade through the spot at the focal point. A beam splitter was oriented between the shutter and the aperture such that the probe beam was collinear with the pump beam and the probe spot fell on a bright fringe in the sample when the crystal was rotated close to the Bragg angle for the 488 nm light. For the data reported here, the angle of incidence is $\sim 1°$ greater than the Bragg angle. Under these

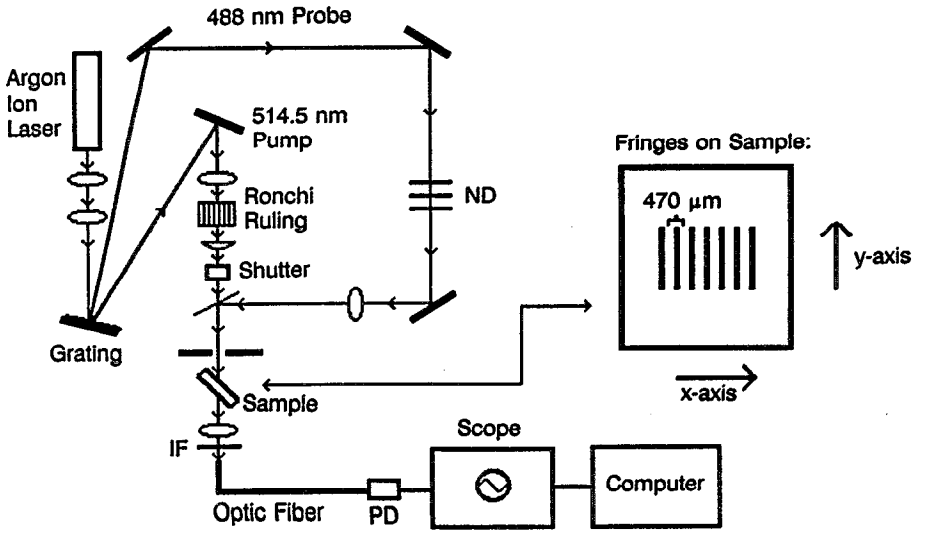

FIG. 1. A schematic of the experimental apparatus. The inset schematically shows the fringe pattern on the sample.

conditions, the probe beam spot fell on the inner edge of the projected Kossel ring deriving from the bcc (110) planes, and a thermally induced local compression decreases the transmitted probe beam intensity while relaxation results in a transmitted intensity increase.

The transmitted probe light was collected with a condensing lens and focused onto a 1 mm diam. optic fiber coupled to a Hamamatsu S1226-18BQ photodiode. An interference filter was placed prior to the optic fiber to limit the detected intensity to the 488 nm light. The measured time-dependent transmitted intensity was stored in a Hewlett–Packard model 54201A digitizing oscilloscope, which was operated in single shot mode and was triggered by the electronic shutter. Opening the shutter to allow the pump beam fringe pattern to fall on the sample triggered the oscilloscope, but collection was delayed to begin when the shutter closed. A background was collected prior to each data set under identical conditions, except that the pump beam was physically blocked. The digitized data was downloaded to a computer for analysis.

The ambient temperature for these measurements was 23.5 °C. At this temperature, we did not observe the initial crystal expansion measured in previous studies at 18.5 °C.[38,39] The pump intensities used are sufficiently low that we can neglect particle motion due to photophoresis, thermophoresis, and radiation pressure.[39] In addition, we did not observe any transmitted intensity changes for the crystal prepared with undyed polystyrene spheres.[38]

RESULTS AND DISCUSSION

A particle concentration gradient is created via local compression of the crystals in the high pump beam intensity (high temperature) regions. This compression derives from the decrease of the interparticle repulsive interaction in these hot regions relative to the surrounding colder regions not illuminated. The pump light is incident on the crystal as a one-dimensional periodic array of bright fringes resulting in a periodic concentration grating. As will be discussed below, the relaxation time constant of this one-dimensional concentration grating is simply related to the collective diffusion coefficient. In our previous work with the thermally induced local compression of colloidal crystals, we found that a portion of the crystal relaxation can be fit to a single exponential.[38] However, since relaxation occurred in three dimensions, the relaxation time constant is not simply related to the collective diffusion coefficient.

We assume a screened Coulomb interparticle repulsive interaction. For two spheres separated by a distance r, the interaction potential can be written as[1]

$$U(r) = \frac{Z^2 e^2}{\epsilon}\left(\frac{e^{\kappa a}}{1+\kappa a}\right)^2 \frac{e^{-\kappa r}}{r}, \tag{5}$$

where Z is the number of charges per sphere, e is the electronic charge, and a is the sphere radius. The temperature-dependent dielectric constant ϵ is taken to be that of water since the volume fraction of polystyrene is only $\sim 2\%$. The reciprocal Debye double layer thickness κ is given by[1]

$$\kappa^2 = \frac{4\pi e^2}{\epsilon k_B T}(n_p Z + n_i), \tag{6}$$

where n_p is the particle number density and n_i is the ionic impurity concentration [as in our previous work, we assume that $n_i = n_p Z$ (Refs. 12, 38, 39)]. If the temperature increase is localized, particles will migrate from the adjacent lower temperature regions to the locally hotter regions due to the force created by a gradient in the interaction potential, resulting in a particle concentration pattern which mimics the pump intensity profile. Particle motion depends on the particle number density, the interaction potential and its temperature derivative, and on the Debye double layer thickness and its temperature derivative.[39] Since the pump intensity is a one-dimensional periodic grating of bright fringes, the particle concentration profile will also be a one-dimensional periodic array of high- and low-particle number density. The periodic array of bright fringes extends across a large portion of the crystal; the height of the fringes are much greater than the diameter of the probe beam. When the pump intensity pattern is turned off, the magnitude of the interaction potential within the heated (illuminated) regions increases, achieving thermal equilibration within ~ 0.1 s. The particle concentration grating relaxes by particle motion predominantly in one dimension along the grating axis towards a uniform particle number density.

The rate of relaxation of the grating is given by Fick's law, which can be written as[43]

$$\frac{\partial n}{\partial t} = D_c \nabla^2 n. \tag{7}$$

Here, the pump intensity distribution is assumed to be sinusoidal in the x direction and n is considered to be

$$n = n_t \sin\left(\frac{2\pi}{\Delta} x\right) + n_p, \tag{8}$$

where x is defined as the direction along the grating axis (see Fig. 1), Δ is the spatial period of the intensity and concentration gratings, D_c is the collective diffusion coefficient, and n_p is the average particle number density (9.28×10^{13} cm^{-3}). A solution to this differential equation is

$$n_t = n_m e^{-t/\tau_p}, \tag{9}$$

where n_m is the excess particle number density over n_p in the center of the heated region (at the position of the probe beam) when the pump beam is turned off and τ_p is the crystal relaxation time constant, which is related to the collective diffusion coefficient by[21,44,45]

$$\tau_p = \frac{\Delta^2}{4\pi^2 D_c}. \tag{10}$$

Thus, we expect the particle concentration grating to relax as a single exponential decay.

The change in the transmitted intensity is linearly proportional to the change in particle number density close to the diffraction condition.[39] Therefore, the transmitted intensity should also change as a single exponential with the same time constant τ_p, and since the initial condition is such that the angle of incidence of the probe beam is slightly

greater than the Bragg angle, the transmitted intensity should increase upon crystal relaxation.

The collective diffusion coefficient is related to the long wavelength limit of the static structure factor $S(0)$ by[46,47]

$$D_c = \frac{D_0(1-6\phi)}{S(0)}, \tag{11}$$

where D_0 is the free particle self-diffusion coefficient. The factor $(1-6\phi)$ in the numerator accounts for hydrodynamic interactions.[48] In the limit $q \to 0$, the static structure factor is related to the elastic modulus of the crystal[46]

$$S(0) = \frac{E}{n_p k_B T}. \tag{12}$$

The elastic modulus E is given by[49]

$$E = B + \tfrac{4}{3}C, \tag{13}$$

where the bulk B and shear C moduli for a bcc colloidal crystal are given by

$$B = \tfrac{4}{9} n_p (\kappa r + 2)^2 U(r) \tag{14}$$

and

$$C = \tfrac{4}{9} n_p (\kappa r)^2 U(r). \tag{15}$$

Therefore, measurement of the crystal relaxation time constant, under conditions of one-dimensional diffusion, unambiguously characterizes the collective diffusion coefficient.

Figure 2 shows the relaxation data collected for the dyed crystal after illumination by the pump intensity pattern for 60 s. The pump power density per bright fringe was 2.6×10^{-2} W/cm^2. The background is also included in this plot to show that the transmitted intensity does not change unless the crystal is first illuminated with the pump beam. The data are reproducible within experimental error.

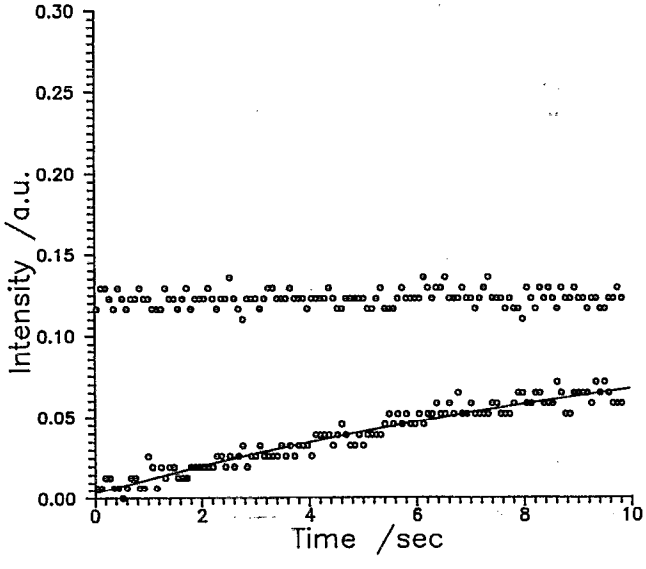

FIG. 2. Crystal relaxation data for a pump duration of 60 s with a power density of 2.6×10^{-2} W/cm^2/fringe. The solid line through the data is the two-parameter fit with a relaxation time constant of $\tau_p = 16.5$ s. The data above the relaxation curve is the background, collected under the same experimental conditions, except the pump beam is blocked prior to the sample.

The solid line through the data is a two-parameter nonlinear least-squares fit using the model

$$y = a - be^{-t/\tau_p} \tag{16}$$

with fitting parameters a and b. τ_p for this crystal was calculated to be 16.5 s using Eqs. (11)–(15) from the Coulomb pair interaction potential given by Eqs. (5) and (6). For this calculation, we assumed[12,39] that the impurity concentration was $n_p Z$ and we used the renormalized surface charge number of 1150.[50] The agreement with the data is quite good. We also performed a three-parameter fit [where $c = 1/\tau_p$ is the third parameter in Eq. (16)]. From this three-parameter fit, the relaxation time constant τ_p was determined to be 16.3 s, which is in good agreement with the calculated value. The best estimates of the parameters of the two- and three-parameter fits for this data set are listed in Table I.

Figure 3 shows relaxation data collected at a higher fringe power density (4.5×10^{-2} W/cm^2) for different pump durations corresponding to 30 and 60 s for Figs. 3(a) and 3(b), respectively. These sets overlap within experimental error suggesting that the crystal is reaching steady state in response to the temperature perturbation within 30 s. The solid lines through these data sets are again the two-parameter best fits with $\tau_p = 16.5$ s. The best fit estimates of the parameters and the errors are listed in Table II.

Figure 4 shows data collected at even higher pump power densities (6.4×10^{-2} W/cm^2) and for pump durations of 15 and 30 s, respectively. These data do not overlap and we suspect that the first 15 s pump annealed the heated regions of the crystal resulting in the improved signal for the 30 s pump data, which was collected next. In addition, using a relaxation time constant of 16.5 s results in a poor fit to the data. If τ_p is decreased to 5 s, however, the fit improves. The parameters and errors for these data are listed in Table III.

At this time we do not understand the decrease in the relaxation time constant for the highest intensity data and, consequently, the apparent increase in the collective diffusion coefficient [Eq. (10)]. We suspect that the decrease in relaxation time constant with increasing incident pump intensity is due to a breakdown in the one-dimensional diffusion condition. If the spheres are not constrained to move only in one direction, then the relaxation of the concentration gradient will be faster due to the additional diffusion in other directions.

The signal-to-noise ratio for these measurements is a function of the crystal quality. A well-ordered crystal gives

TABLE I. Fitting parameters for 2.6×10^{-2} W/cm^2/fringe pump intensity, 60 s pump duration.

	a	b	c $(=1/\tau_p)$
Two parameter	0.14 ± 0.0026	0.14 ± 0.0034	⋯
Three parameter	0.14 ± 0.033	0.14 ± 0.032	0.061 ± 0.019

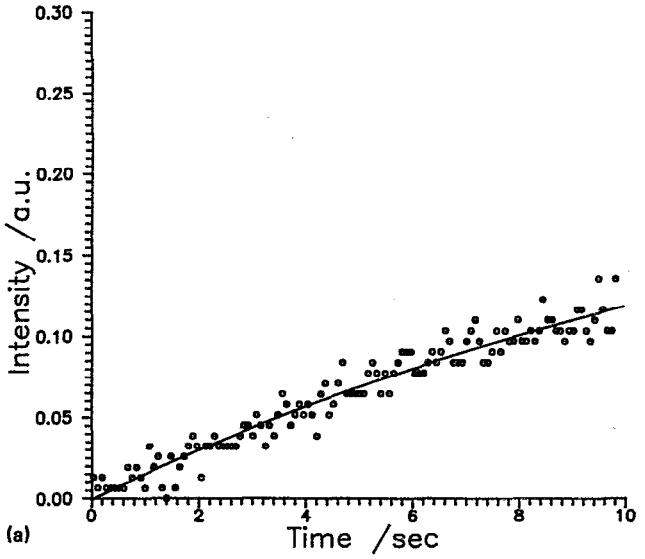

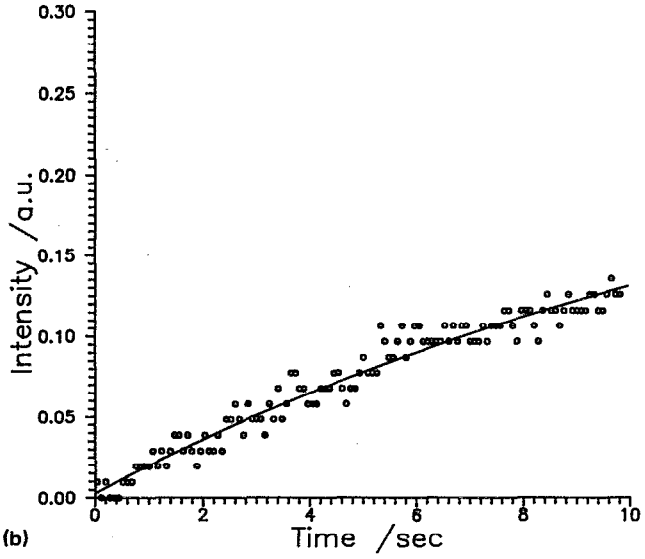

FIG. 3. Crystal relaxation data with a pump power density of 4.5×10^{-2} W/cm^2/fringe for pump durations of (a) 30 and (b) 60 s, respectively. The solid lines through the data are the two-parameter fits with the relaxation time constant τ_p of 16.5 s.

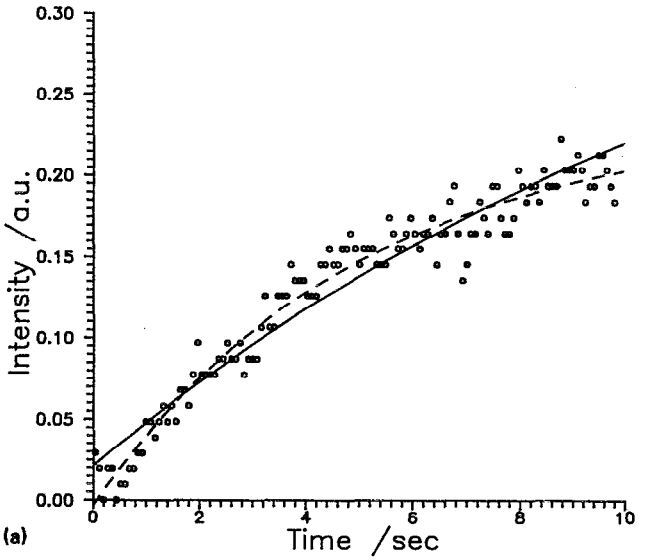

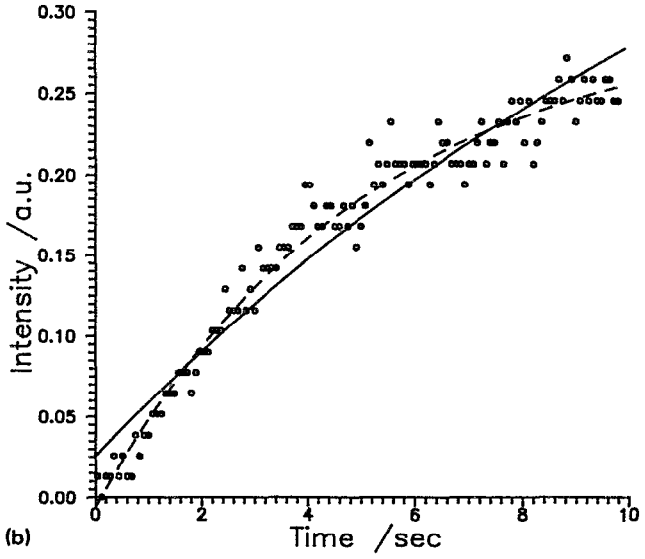

FIG. 4. Crystal relaxation data with a pump power density of 6.4×10^{-2} W/cm^2/fringe for pump durations of (a) 15 and (b) 30 s, respectively. The solid lines through the data are the two-parameter fits with $\tau_p = 16.5$ s and the dashed lines correspond to $\tau_p = 5$ s.

rise to a sharp, well-defined Kossel ring and small changes in the ring diameter when the diffraction conditions are almost satisfied gives rise to a large change in the transmitted probe intensity. On the other hand, as the crystal defect density increases, the Kossel ring becomes more diffuse and the contrast between the ring and the surroundings decreases. Changes in the ring diameter in this case do not result in large changes in the transmitted probe intensity. Therefore, the colloidal crystal must be well ordered for this method to be useful for determining the collective diffusion coefficient. We suspect that the low intensity pump results in a small temperature increase which might not be sufficient to anneal

TABLE II. Fitting parameters for 4.5×10^{-2} W/cm^2/fringe pump intensity.

Pump duration (s)	a	b
30	0.26 ± 0.0045	0.26 ± 0.0059
60	0.29 ± 0.0043	0.28 ± 0.0056

TABLE III. Fitting parameters for 6.4×10^{-2} W/cm^2/fringe pump intensity.

Pump duration (s)	τ_p (s)	a	b
15	16.5	0.46 ± 0.0082	0.44 ± 0.011
15	5	0.24 ± 0.0022	0.24 ± 0.0045
30	16.5	0.58 ± 0.010	0.55 ± 0.013
30	5	0.30 ± 0.0023	0.30 ± 0.0047

the crystal. Hence, the low pump intensity relaxation data is reproducible. At higher pump intensities (e.g., 6.5×10^{-2} W/cm^2/fringe), the temperature increase may be sufficient to anneal the crystal. Hence, the signal-to-noise ratio improves at this higher pump intensity. At much higher pump intensities (>0.15 W/cm^2/fringe), the temperature increase is sufficient to disorder the crystal considerably, resulting in a diffuse Kossel ring; this significantly decreases the signal-to-noise ratio for subsequent measurements.

CONCLUSION

We present a new technique to determine the collective diffusion coefficient in colloidal crystals based on the photoinduced compression phenomenon. By illuminating an absorbing colloidal crystal, prepared from an aqueous suspension of dyed polystyrene spheres, with a spatially periodic intensity profile, a particle concentration grating is created which follows the intensity pattern of the pump light. Since diffusion is constrained to primarily one dimension under these conditions, the collective diffusion coefficient is determined easily from the relaxation time constant of this concentration grating. The measured collective diffusion coefficient agrees closely with the calculated value assuming a screened Coulomb repulsive pair interaction.

[1] D. Thirumalai, J. Phys. Chem. **93**, 5637 (1989).
[2] R. Kesavamoorthy, B. V. R. Tata, A. K. Arora, and A. K. Sood, Phys. Lett. A **138**, 208 (1989).
[3] W. Y. Shih, I. A. Aksay, and R. Kikuchi, J. Chem. Phys. **86**, 5127 (1987).
[4] D. Hone, S. Alexander, P. M. Chaikin, and P. Pincus, J. Chem. Phys. **79**, 1474 (1983).
[5] H. M. Lindsay and P. M. Chaikin, J. Chem. Phys. **76**, 3774 (1982).
[6] D. W. Schaefer, J. Chem. Phys. **66**, 3980 (1977).
[7] Y. Monovoukas and A. P. Gast, J. Colloid Interface Sci. **128**, 533 (1989).
[8] M. O. Robbins, K. Kremer, and G. S. Grest, J. Chem. Phys. **88**, 3286 (1988).
[9] W. Shih and D. Stroud, J. Chem. Phys. **79**, 6254 (1983).
[10] R. Williams, R. S. Crandall, and P. J. Wojtowicz, Phys. Rev. Lett. **37**, 348 (1976).
[11] W. B. Russel, D. A. Saville, and W. R. Schowalter, *Colloidal Dispersions* (Cambridge University, New York, 1989).
[12] P. A. Rundquist, R. Kesavamoorthy, S. Jagannathan, and S. A. Asher, J. Chem. Phys. **95**, 1249 (1991).
[13] P. A. Rundquist, P. Photinos, S. Jagannathan, and S. A. Asher, J. Chem. Phys. **91**, 4932 (1989).
[14] R. J. Spry and D. J. Kosan, Appl. Spectrosc. **40**, 782 (1986).
[15] P. A. Hiltner and I. M. Krieger, J. Phys. Chem. **73**, 2386 (1969).
[16] S. A. Asher, P. L. Flaugh, and G. Washinger, Spectroscopy **1**, 26 (1986).
[17] P. L. Flaugh, S. E. O'Donnell, and S. A. Asher, Appl. Spectrosc. **38**, 847 (1984).
[18] S. A. Asher, U. S. Patents Nos. 4,627,689 and 4,632,517.
[19] B. J. Berne and R. Pecora, *Dynamic Light Scattering* (Wiley, New York, 1976).
[20] M. Venkatesan, C. S. Hirtzel, and R. Rajagopalan, J. Chem. Phys. **82**, 5685 (1985).
[21] W. D. Dozier, H. M. Lindsay, and P. M. Chaikin, J. Phys. (Paris) Colloq. C **3**, 165 (1985).
[22] C. M. Trotter and D. N. Pinder, J. Chem. Phys. **75**, 118 (1981).
[23] J. A. Marqusee and J. M. Deutch, J. Chem. Phys. **73**, 5396 (1980).
[24] X. Qiu, H. D. Ou-Yang, D. J. Pine, and P. M. Chaikin, Phys. Rev. Lett. **61**, 2554 (1988).
[25] X. Qiu, D. Ou-Yang, and P. M. Chaikin, J. Phys. (Paris) **49**, 1043 (1988).
[26] B. J. Ackerson and A. H. Chowdbury, Faraday Discuss. Chem. Soc. **83**, 309 (1987).
[27] S. Fraden, A. J. Hurd, and R. B. Meyer, Phys. Rev. Lett. **63**, 2373 (1989).
[28] T. Okubo, J. Chem. Soc. Faraday Trans. I **83**, 2487 (1987).
[29] M. Tomita and T. G. M. van de Ven, J. Phys. Chem. **89**, 1291 (1985).
[30] R. Kesavamoorthy and A. K. Arora, J. Phys. A **18**, 3389 (1985).
[31] R. J. Carlson and S. A. Asher, Appl. Spectrosc. **38**, 297 (1984).
[32] R. S. Crandall and R. Williams, Science **198**, 293 (1977).
[33] T. Okubo, J. Am. Chem. Soc. **112**, 5420 (1990).
[34] C. Mathis, G. Bossis, and J. F. Brady, J. Colloid Interface Sci. **126**, 16 (1988).
[35] B. J. Ackerson, in *Physics of Complex and Supermolecular Fluids*, edited by N. A. Clark and S. Safran, (Wiley-Interscience, New York, 1987), p. 553.
[36] M. Tomita and T. G. M. van de Ven, J. Colloid Interface Sci. **99**, 374 (1984).
[37] N. A. Clark, A. J. Hurd, and B. J. Ackerson, Nature **281**, 57 (1979).
[38] P. A. Rundquist, S. Jagannathan, R. Kesavamoorthy, C. Brnardic, S. Xu, and S. A. Asher, J. Chem. Phys. **94**, 711 (1991).
[39] R. Kesavamoorthy, S. Jagannathan, P. A. Rundquist, and S. A. Asher, J. Chem. Phys. **94**, 5172 (1991).
[40] D. W. Schaefer, J. Chem. Phys. **66**, 3980 (1977).
[41] P. A. Hiltner, Y. S. Papir, and I. M. Krieger, J. Phys. Chem. **75**, 1881 (1971).
[42] J. B. Bateman, E. J. Weneck, and D. C. Eshler, J. Colloid Sci. **14**, 308 (1959).
[43] P. C. Hiemenz, *Principles of Colloid and Surface Chemistry*, 2nd ed. (Dekker, New York, 1986).
[44] B. A. Smith and H. M. McConnell, Proc. Natl. Acad. Sci. USA **75**, 2759 (1978).
[45] H. Eichler, G. Salje, and H. Stahl, J. Appl. Phys. **44**, 5383 (1973).
[46] F. Grüner and W. P. Lehmann, J. Phys. A **15**, 2847 (1982).
[47] P. N. Pusey and R. J. A. Tough, in *Dynamic Light Scattering: Applications of Photon Correlation Spectroscopy*, edited by R. Pecora (Plenum, New York, 1985), p. 85–179.
[48] B. J. Ackerson, J. Chem. Phys. **64**, 242 (1976).
[49] R. Kesavamoorthy and A. K. Arora, J. Phys. C **19**, 2833 (1986).
[50] S. Alexander, P. M. Chaikin, P. Grant, G. J. Morales, P. Pincus, and D. Hone, J. Chem. Phys. **80**, 5776 (1984).